

University of Nebraska - Lincoln

## DigitalCommons@University of Nebraska - Lincoln

---

Faculty Publications: Materials Research  
Science and Engineering Center

Materials Research Science and Engineering  
Center

---

7-1-2004

### Domain-Wall Pinning at Inhomogeneities of Arbitrary Cross-Sectional Geometry

Ralph Skomski

*University of Nebraska-Lincoln*, rskomski2@unl.edu

Jian Zhou

*University of Nebraska - Lincoln*

Arti Kashyap

*University of Nebraska-Lincoln*, akashyap@lnmiit.ac.in

David J. Sellmyer

*University of Nebraska-Lincoln*, dsellmyer@unl.edu

Follow this and additional works at: <https://digitalcommons.unl.edu/mrsecfacpubs>



Part of the [Materials Science and Engineering Commons](#)

---

Skomski, Ralph; Zhou, Jian; Kashyap, Arti; and Sellmyer, David J., "Domain-Wall Pinning at Inhomogeneities of Arbitrary Cross-Sectional Geometry" (2004). *Faculty Publications: Materials Research Science and Engineering Center*. 21.

<https://digitalcommons.unl.edu/mrsecfacpubs/21>

This Article is brought to you for free and open access by the Materials Research Science and Engineering Center at DigitalCommons@University of Nebraska - Lincoln. It has been accepted for inclusion in Faculty Publications: Materials Research Science and Engineering Center by an authorized administrator of DigitalCommons@University of Nebraska - Lincoln.

# Domain-Wall Pinning at Inhomogeneities of Arbitrary Cross-Sectional Geometry

Ralph Skomski, Jian Zhou, Arti Kashyap, and David J. Sellmyer

**Abstract**—The coercivity of cellular Sm-Co based permanent magnets is investigated by model calculations. The grain boundaries responsible for the pinning coercivity are modeled as planar inhomogeneities with arbitrary cross-sectional geometry. The calculation yields a physically transparent integral equation for the pinning energy, whose derivative is the pinning force. The theory rationalizes experimental data on a semiquantitative level, but without adjustable parameters, and bridges the gap between smooth concentration gradients and abrupt interfaces. Explicit results are obtained for sinusoidal profiles, for very thin grain boundaries, and for profiles intermediate between attractive and repulsive pinning. The corrections predicted by the present model elucidate the occurrence of coercivity when the main and grain-boundary phases have the same wall energy.

**Index Terms**—Coercive force, magnetic anisotropy, magnetic films, permanent magnets, samarium alloys.

## I. INTRODUCTION

**P**INNING-TYPE Sm-Co magnets, first developed in the 1970s [1]–[3], [22], have attracted renewed attention as permanent magnet materials for high-temperature applications [4]–[12]. Industrial pinning-type Sm-Co magnets [1]–[3], [22] consist of regions of the main phase (essentially  $\text{Sm}_2\text{Co}_{17}$ ) surrounded by a grain boundary phase (essentially  $\text{SmCo}_5$ ). The coercivity of these magnets reflects chemical composition fluctuations, which translate into inhomogeneous profiles of intrinsic properties. For example, a variation of the elemental composition across grain boundaries has been observed by energy-dispersive X-ray diffraction (EDX) microanalysis [5].

The leading contribution is usually from the anisotropy; exchange stiffness and spontaneous magnetization tend to be less inhomogeneous. The pinning occurs at grain boundaries, and the energy barriers responsible for coercivity are, in crude approximation, proportional to  $K_1(1:5) - K_1(2:17)$ . Fig. 1 shows typical anisotropy profiles. Depending on whether the anisotropy of the 1:5 grain-boundary phase is lower or higher than that of the main 2:17 phase, one encounters attractive pinning, as in Fig. 1(a), or repulsive pinning, as in Fig. 1(b). By adjusting the chemical composition [3] or, for some compositions, the temperature [4], it is possible to tune the anisotropies of the two phases.

A key problem is to derive the coercivity from the variation of the micromagnetic parameters, that is, essentially, from the

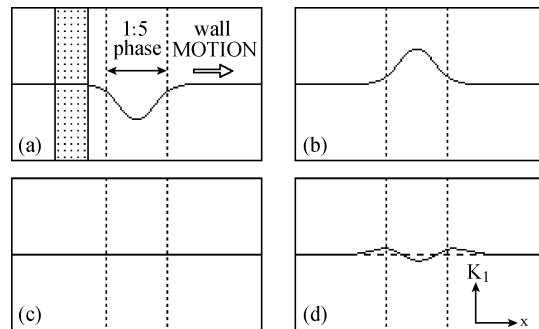


Fig. 1. Pinning energy at a grain boundary phase: (a) attractive pinning, (b) repulsive pinning, (c) no pinning, and (d) “residual” pinning.  $K_1(x)$  reflects the local chemistry.

anisotropy profiles. Various concentration profiles, such as slow variations and steps, have been used in micromagnetic simulations and in model calculations [9], [13], but these calculations assume simplistic concentration profiles and produce results that are difficult to compare with experiment. Here we consider the coercivity caused by arbitrary anisotropy profiles.

## II. MICROMAGNETIC BACKGROUND

Pinning is encountered in strongly inhomogeneous magnets and means that the coercivity is determined by the interaction of domain walls with structural inhomogeneities [13]–[15]. As in other areas of micromagnetics, the starting point of the consideration is the field-dependent micromagnetic (free) energy [16]–[18], which depends on the spontaneous magnetization  $M_s$ , on the exchange stiffness  $A$ , on the first uniaxial anisotropy constant  $K$ , and on the unit vector  $\mathbf{n}$  determining the easy axis. These parameters are all *local* parameters, because they depend on the local chemistry, crystal structure, and crystallite orientation.

From the micromagnetic energy, the local magnetization  $\mathbf{M}(\mathbf{r})$  is obtained by tracing minima of  $E$  as a function of the external field. When the spatial variation of the anisotropy is sufficiently smooth, then the well-known equation [14]

$$E = \gamma(x) - 2\mu_0 M_s H x_0 \quad (1)$$

can be used, where  $\gamma = 4(AK)^{1/2}$  is the domain-wall energy per wall area. Taking the derivative of this equation with respect to  $x$  yields the  $H = d\gamma(x)/dx/2\mu_0 M_s$ , and the maximum of  $H$  is the pinning coercivity. However, the applicability of this macroscopic approach is limited, because the domain-wall width  $\delta_B$  is usually comparable to or larger than the thickness  $b$  of the grain-boundary region. Note, furthermore, that the consideration of the coercivity as a derivative of the micromag-

Manuscript received October 16, 2003. This work was supported by AFOSR, DOE, NSF MRSEC, the Keck Foundation, and CMRA.

The authors are with the Department of Physics and Astronomy and Center for Materials Research and Analysis, University of Nebraska, Lincoln, NE 68588 USA (e-mail: rskomski@unlserve.unl.edu; jzhou@unlserve.unl.edu; akashyap2@unl.edu; dsellmyer@unl.edu).

Digital Object Identifier 10.1109/TMAG.2004.832163

netic free energy is a static approach. It does not account for the finite-temperature dynamics of the coercivity, but the corresponding sweep-rate correction is small and can usually be ignored [18].

Another simple expression exists for small planar inhomogeneities with rectangular cross section. For an inhomogeneity of anisotropy  $K = K_o + \Delta K$  and thickness  $b$ , the pinning coercivity is

$$H_c = H_a \frac{\pi b}{3\sqrt{3}\delta_B} \frac{|\Delta K|}{K_o} \quad (2)$$

where  $\delta_B = \pi(A/K_o)^{1/2}$  is the Bloch-wall width of the main phase and  $H_a = 2K/\mu_o M_s$ . In the context of magnetostrictive anisotropy, (2) was first derived in the 1930s [14].

### III. CALCULATION AND RESULTS

For the calculation, we assume that the grain boundary lies in the  $y$ - $z$  plane. In the limit of weak inhomogeneities, the domain-wall fine structure remains unperturbed. The wall is then described the position  $x_o$  of its center, and the pinning energy is obtained by straightforward integration.

The spin structure of a Bloch wall in the  $y$ - $z$  plane is

$$\mathbf{M} = M_s m e_z + \sqrt{1 - m^2} M_s e_y \quad (3)$$

where  $m(x) = \tanh((x - x_o)/\delta_o)$  and  $\delta_o = \delta_B/\pi$  is the wall-width parameter of the unperturbed or ‘‘rigid’’ wall [17]. Using (3) to calculate the micromagnetic energy for an arbitrary anisotropy profile yields

$$E(x_o) = 2 \int K(x) \left( 1 - \tanh^2 \left( \frac{(x - x_o)}{\delta_o} \right) \right) dx - 2\mu_o M_s H x_o. \quad (4a)$$

By exploiting  $\tanh'(x) = 1 - \tanh^2(x)$  and  $(a(x)b(x))' = a'(x)b(x) + a(x)b'(x)$ , we can also write

$$E(x_o) = -2 \int K'(x) \tanh \left( \frac{(x - x_o)}{\delta_o} \right) dx - 2\mu_o M_s H x_o. \quad (4b)$$

These two equations are equivalent but reflect slightly different interpretation of domain-wall pinning. In (4a), pinning is interpreted as an interaction of a magnetization gradient with an anisotropy inhomogeneity, whereas in (4b) the magnetization interacts with the anisotropy gradient.

From (4), the pinning field is obtained by evaluating the derivative of  $E$  with respect to  $x_o$ . Fig. 2 shows the resulting coercivity for a sinusoidal variation of the anisotropy,  $K(x) = K_o + \Delta K \sin(2\pi x/\lambda)$ . The coercivity exhibits a maximum when the wavelength of the inhomogeneity becomes comparable to the wall width. For long-wavelength inhomogeneities the pinning force is small, because wall-energy gradient  $d\gamma/dx$  goes to zero. In the opposite limit of rapidly oscillating inhomogeneities, the pinning force is reduced due to averaging over a distance of order  $\delta_B$ . In a slightly different context [13], [17], this regime is known as weak pinning. The coercivity maximum occurs at  $\lambda = 1.64\delta_B$ , and the corresponding coercivity is  $1.41 \Delta K/\mu_o M_s$ . Since the domain-wall widths of  $\text{Sm}(\text{CoCu})_5$  and  $\text{Sm}_2(\text{CoT})_{17}$  are of the order of 5 nm,

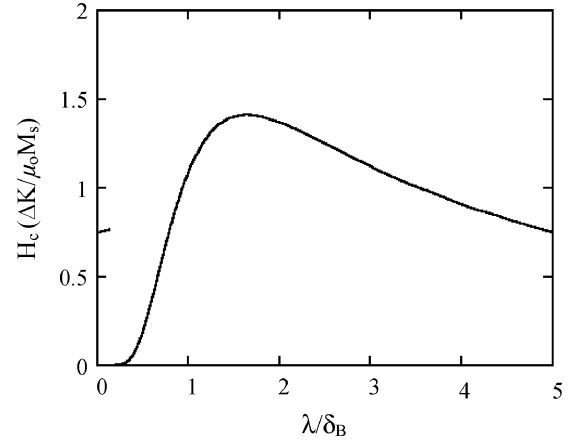


Fig. 2. Pinning due to a sinusoidal anisotropy inhomogeneity of wavelength  $\lambda$ .

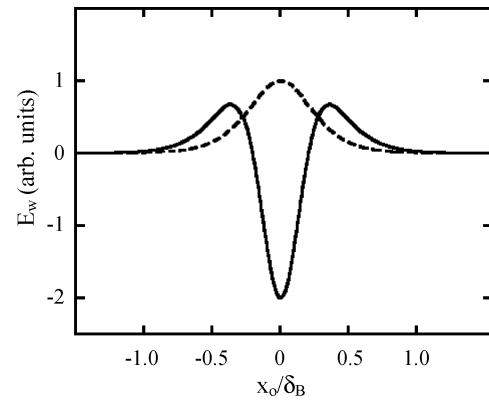


Fig. 3. Energy landscape describing the pinning due to a well-localized planar defect. The functional structures of the curves are  $1 - \tanh^2(x_o/\delta_o)$  for lowest-order pinning (dashed line) and  $\delta_o^3 d^3 \tanh(x_o/\delta_o)/dx^3$  for second-order pinning (solid line).

very smooth (sinoidal) concentration profiles maximize the coercivity when the modulation wavelength is about 8.2 nm.

A relatively simple solution is also obtained for very thin grain boundaries of arbitrary cross section. This case is only occasionally encountered in practice, but it provides insight into nanoscale deviations from the macroscopic picture of (1). The pinning potential is obtained by expanding the hyperbolic tangents in (4) into powers of the distance between wall and pinning inhomogeneity. The problem then reduces to the consideration of the moments  $\langle x^m \Delta K(x) \rangle$  characterizing the pinning strength of the inhomogeneity.

For  $\langle \Delta K(x) \rangle \neq 0$  one encounters attractive or repulsive pinning, depending on whether the sign of the zeroth moment is negative or positive, respectively. For  $\langle \Delta K(x) \rangle = 0$ , as in Fig. 1(c) and (d), higher moments become important. The first moment,  $\langle xK(x) \rangle$ , vanishes for symmetric grain boundaries, but there is some residual pinning associated with the second moment  $\langle x^2 \Delta K(x) \rangle$ . This explains why profiles such as that in Fig. 1(d) yield nonzero coercivity, in spite of the fact that the average anisotropies of the main and grain-boundary phases are equal. The second-moment pinning contribution scales as  $(b/\delta_B)^2$ , strongly decreasing with grain-boundary thickness  $b$ . When  $b$  is comparable to or larger than  $\delta_B$ , higher-order moments must be included, but the qualitative picture remains the

same. Based on these considerations, we estimate that the coercivity in the regime of Fig. 1(d) is  $6 (\pm 3)$  times lower than those in regimes of Fig. 1(a) and (b), in fair agreement with experiment.

Fig. 3 shows the pinning energies for  $\langle \Delta K(x) \rangle \neq 0$  (dashed line) and  $\langle \Delta K(x) \rangle = 0$  (solid line). It is important to note that the shape of the energy landscape reflects the domain-wall fine structure but is *independent* of the details of  $K(x)$ . This is contrast to the limit of smooth extended boundaries, where (1) applies and details of  $K(x)$  are important.

#### IV. DISCUSSION AND CONCLUSIONS

The present theory relies on three main assumptions. First, we have assumed that the pinning reflects inhomogeneities of the anisotropy constant. This is a fair assumption, because other inhomogeneities, such as exchange inhomogeneities, are often less pronounced and tend to have a disproportionately small effect on micromagnetic properties [4], [19]. Second, we have made the physically transparent but idealized assumption of a planar domain wall. Domain-wall curvature is generally nonnegligible, but their discussion [20], [21] goes beyond the scope of this paper.

Finally, we have assumed that the magnitude and extension of the inhomogeneity are small. This assumption is unrealistic in many cases but yields only moderate corrections. Extended defects, as well as defects where  $\Delta K$  is comparable to  $K_0$ , mean that the domain-wall structure adjusts to the  $K(x)$  profile and the "rigid-wall" approximation of Section III becomes inadequate. For example,  $\delta_0 = \delta_B/\pi$  in (4) can no longer be considered as a constant. It can be shown that this effect reduces the coercivity, and in the long-wavelength limit ( $\lambda = \infty$  in Fig. 2) the reduction is by a factor of two.

In conclusion, we have developed a semiquantitative theory to describe pinning at planar inhomogeneities of arbitrary cross section. These inhomogeneities reflect details of the microchemistry, such as the degree of interdiffusion, and are an essential aspect of the coercivity of pinning-type Sm-Co magnets. Starting from an approximate but closed integral, explicit solutions have been obtained for sinusoidal profiles of different periodicities and for well-localized planar defects. In the case of well-localized defects, the pinning is conveniently described in terms of a moments expansion of the anisotropy inhomogeneity. The zeroth moment is essentially the average anisotropy difference between the grain-boundary and main phases and determines whether the pinning is repulsive and attractive. Higher-order moments are important when the main

and grain-boundary phases have the same average anisotropy and then yield a residual coercivity.

#### REFERENCES

- [1] J. D. Livingston and D. L. Martin, "Microstructure of aged (Co, Cu, Fe)<sub>7</sub>Sm magnets," *J. Appl. Phys.*, vol. 48, pp. 1350–1354, 1977.
- [2] J. Fidler and P. Skalicky, "Microstructure of precipitation hardened cobalt rare earth permanent magnets," *J. Magn. Magn. Mater.*, vol. 27, pp. 127–134, 1982.
- [3] K. Kumar, "RETM<sub>5</sub> and RE<sub>2</sub>TM<sub>17</sub> permanent magnets development," *J. Appl. Phys.*, vol. 63, pp. R13–R57, 1988.
- [4] J. Zhou, R. Skomski, C. Chen, G. C. Hadjipanayis, and D. J. Sellmyer, "Sm-Co-Ti high-temperature permanent magnets," *Appl. Phys. Lett.*, vol. 77, pp. 1514–1516, 2000.
- [5] D. Goll, I. Kleinschroth, W. Sigle, and H. Kronmüller, "Melt-spun precipitation-hardened Sm<sub>2</sub>(Co, Cu, Fe, Zr)<sub>17</sub> magnets with abnormal temperature dependence of coercivity," *Appl. Phys. Lett.*, vol. 76, pp. 1054–1056, 2000.
- [6] G. C. Hadjipanayis, W. Tang, Y. Zhang, S. T. Chui, J. F. Liu, C. Chen, and H. Kronmüller, "High temperature 2:17 magnets: relationship of magnetic properties to microstructure and processing," *IEEE Trans. Magn.*, vol. 36, no. 5, pp. 3382–3387, 2000.
- [7] S. Liu, J. Yang, G. Doyle, G. Potts, and G. E. Kuhl, "Abnormal temperature dependence of intrinsic coercivity in sintered Sm-Co-based permanent magnets," *J. Appl. Phys.*, vol. 87, pp. 6728–6730, 2000.
- [8] M. Q. Huang, W. E. Wallace, M. McHenry, Q. Chen, and B. M. Ma, "Structure and magnetic properties of SmCo<sub>0.7-x</sub>Zr<sub>x</sub> alloys ( $x = 0 - 0.8$ )," *J. Appl. Phys.*, vol. 83, pp. 6718–6720, 1998.
- [9] H. R. Hilzinger and H. Kronmüller, "Investigation of Bloch wall pinning by antiphase boundaries in RCo<sub>5</sub> compounds," *Phys. Lett. A*, vol. 51, pp. 59–60, 1975.
- [10] C. H. Chen, M. S. Walmer, M. H. Walmer, S. Liu, E. Kuhl, and G. Simonet, "Sm<sub>2</sub>(Co, Fe, Cu, Zr)<sub>17</sub> magnets for use at temperature  $\geq 400^\circ\text{C}$ ," *J. Appl. Phys.*, vol. 83, pp. 6706–6708, 1998.
- [11] J. Zhou, R. Skomski, and D. J. Sellmyer, "Coercivity of titanium-substituted high-temperature permanent magnets," *IEEE Trans. Magn.*, vol. 37, pp. 2518–2520, 2001.
- [12] O. Gutfleisch *et al.*, *Appl. Phys. Lett.*, vol. 83, pp. 2208–2210, 2003, to be published.
- [13] D. Givord and M. F. Rossignol, *Rare-Earth Iron Permanent Magnets*, J. M. D. Coey, Ed. Oxford, U.K.: Oxford Univ. Press, 1996, p. 218.
- [14] R. Becker and W. Döring, *Ferromagnetismus*. Berlin, Germany: Springer, 1939.
- [15] M. Kersten, "Zur Theorie der ferromagnetischen Hysterese und der Anfangspermeabilität," *Z. Phys.*, vol. 44, pp. 63–77, 1943.
- [16] W. F. Brown, "Thermal fluctuations of a single-domain particle," *Phys. Rev.*, pp. 1677–1686, 1963.
- [17] R. Skomski and J. M. D. Coey, *Permanent Magnetism*. Bristol, U.K.: Inst. Physics, 1999.
- [18] R. Skomski, "Nanomagnetics," *J. Phys.: Condens. Matter*, vol. 15, pp. R841–R896, 2003.
- [19] R. Skomski and J. M. D. Coey, "Giant energy product in nanostructured two-phase magnets," *Phys. Rev. B*, vol. 48, pp. 15 812–15 816, 1993.
- [20] R. Skomski, "Domain-wall curvature and coercivity in pinning-type Sm-Co-magnets," *J. Appl. Phys.*, vol. 81, pp. 5627–5629, 1997.
- [21] B. Streibl, J. Fidler, and T. Schrefl, "Domain wall pinning in high temperature Sm(Co, Fe, Cu, Zr)<sub>7-8</sub> magnets," *J. Appl. Phys.*, vol. 87, pp. 4765–4767, 2000.
- [22] J. Fidler, "Coercivity of precipitation hardened cobalt rare earth 17:2 permanent magnets," *J. Magn. Magn. Mater.*, vol. 30, pp. 58–70, 1982.